CHEMISTRY
A EUROPEAN JOURNAL

Isomeric Mono- and Bis[(phosphane)gold(I)] Thiocyanate Complexes

Raphael J. F. Berger,[a] Michael Patzschke,[a] Daniel Schneider,[b] Hubert Schmidbaur,[b] and Dage Sundholm*[a]

Abstract: The solid-state IR spectrum of $Me_3PAuSCN$ shows two signals in the range of the C–N stretching vibrations at 2075 and 2113 cm^{-1}. On the basis of thoroughly tested quantum chemical ab initio calculations (MP2 level of theory) these signals have been assigned to the two isomeric forms $Me_3PAuNCS$ and $Me_3PAuSCN$. The molecular structures, the vibrational frequencies, and the relative energies of the two species have been calculated and the results compared with the experimental IR data. Treatment of $Me_3PAuSCN$ with equimolar quantities of $[(Me_3P)Au]^+[SbF_6]^-$ in CH_2Cl_2 at −78 °C gives the dinuclear reaction product $[C_7H_9Au_2NP_2S]^+[SbF_6]^-$ in high yields. A comparison of results of ab initio calculations and IR data suggest that at least three isomeric cationic species $[(R_3PAu)_2NCS]^+$, $[(R_3PAu)_2SCN]^+$ and $[(R_3PAu)SCN(AuPR_3)]^+$ are present, the second and third being the predominant components. The structures and vibrational frequencies of all three species have been calculated. The relative energies in the gas phase and in solution are discussed and compared with the corresponding data of the experimental IR spectra.

Keywords: ab initio calculations · aurophilicity · gold · IR spectroscopy · quantum chemistry

Introduction

The term *pseudohalogen* suggests a similarity of the general chemical behaviour of this group of species to the halogens. Halide and pseudohalide complexes are by far the most important classes of compounds in gold chemistry.[1,2] For example, the cyanide anion $[CN]^-$ is the key ligand in gold extraction from ores and in gold recycling[3] as well as in surface deposition processes (gilding).[4,5] Based on the observation that the affinity for gold(I) to the thiocyanate anion $[SCN]^-$ is comparable to that for cyanide $[CN]^-$,[6,7] there have been many attempts to replace $[CN]^-$ with $[SCN]^-$ in gold leaching processes, where thiocyanate is expected to have environmental and technological advantages.[3] So far it has not superseded cyanide, though. Gold(I) coordination to the heavier halide ions (excluding fluoride) is also well established and complexes of the type LAuX with X = Cl, Br, I are among the key reagents in gold chemistry. Recent work has shown that these complexes can be converted into digold(I) halogenonium cations of the type $[(LAu)_2X]^+$, where L is a neutral tertiary phosphine ligand.[8–10] Considering the halogen–pseudohalogen analogy, the question arises whether diauration of pseudohalide anions is also possible. In a first series of experiments it was shown that the diauration of the thiocyanate anion can indeed be achieved.[1] While the products could be characterised by elemental analysis, IR and NMR spectroscopy, and mass spectrometry (MS), all attempts to prepare single crystals suitable for X-ray structure analysis have so far been unsuccessful.[1] In the absence of experimental data for structure assignment, the problem was approached using quantum chemical ab initio calculations.

The literature coverage on gold thiocyanate complexes is very extensive. It is mainly concerned with systems where an excess of $[SCN]^-$ is employed for the oxidative complexation of gold metal and mononuclear gold(I) salts, which are particularly relevant as an alternative to cyanide leaching from refractory gold ores. By contrast, the present study is oriented towards systems with an excess of gold(I) in which dinuclear complexes are formed. Schneider et al.[1] recently presented a short summary on gold(I) thiocyanate complexes with phosphino ligands. This also includes some vibrational studies of the $[Au(SCN)_2]^-$ anion, which is not in the focus of the present study.[11]

[a] Dr. R. J. F. Berger, M. Patzschke, Dr. D. Sundholm
Department of Chemistry, P.O. Box 55 (A.I. Virtasen Aukio 1)
00014 University of Helsinki (Finland)
Fax: (+358) 9-191-50169
E-mail: sundholm@chem.helsinki.fi

[b] Dr. D. Schneider, Prof. Dr. H. Schmidbaur
Department Chemie der
Technischen Universität München
Lichtenbergstrasse 4, 85747 Garching (Germany)

DOI: 10.1002/chem.200400916

Treatment of a selection of $(R_3P)AuSCN$ compounds with equimolar quantities of $[(R_3P)Au]BF_4$ or $[(R_3P)Au]SbF_6$ under carefully controlled conditions gave dinuclear adducts of the type $[(R_3PAu)_2SCN]^+Y^-$ in high yields, where R = Ph, 2-Me-C_6H_4, 3-Me-C_6H_4, *i*Pr or Me_2Ph. The general Reaction (1) has been formulated giving preference to the S,S-diaurated structure of the cation, but alternatives could not be ruled out.

$$(R_3P)AuSCN + [(R_3P)Au]^+Y^- \xrightarrow[-78\,^\circ C]{CH_2Cl_2} \{[(R_3P)Au]_2SCN\}^+Y^- \quad (1)$$

In the present study the experimental data are reconsidered and complemented by results obtained from ab initio calculations.

Computational Methods

The present study employs ab initio methods for geometry optimisations on high-dimensional energy surfaces and calculations of vibrational frequencies including anharmonic corrections. Since the dispersion-type *aurophilic* attraction may play an important role for the molecules studied, density-functional-theory (DFT) methods may not be applicable,[12] and because the molecules are large, high-order correlation methods like configuration-interaction (CI) and coupled-cluster (CC) approaches are not feasible. A good compromise regarding accuracy and demands on resources are second-order Møller–Plesset (MP2) perturbation-theory calculations.

Dunning's correlation-consistent double-zeta quality basis sets (cc-pVDZ)[13,14] were used for the lighter elements, while for Au the Stuttgart 60 electron relativistic effective core potential (ECP) and the corresponding double-zeta quality basis set (Stuttgart-RSC-(1997)-ECP)[15] augmented with two f functions were used. The two polarisation f functions with exponents 1.19 and 0.20 are needed for an accurate description of correlation effects and the aurophilic interaction.[16] In the following, this basis set is denoted RDZ, whereas the basis set consisting of the cc-pVDZ basis sets for the lighter elements combined with the original Stuttgart double-zeta basis set for Au is denoted DZ. The applicability of the computational methods was checked by test calculations on $[SCN]^-$ by using calculations up to the coupled-cluster singles and doubles level with a perturbative treatment of triple excitations [CCSD(T)][17–19] and triple-zeta quality basis sets.[13,14] The computational methods were also checked by performing restricted Hartree–Fock (RHF) and MP2 calculations on $[(H_3PAu)_2Cl]^+$ and $R_3PAuSCN$ with R = H, Me. For the latter accurate experimental data are available.

The MP2 geometry optimisations and the harmonic frequency analysis were carried out with the Turbomole[20–22] program package (version 5.6) employing the resolution-of-the-identity (RI) density-fitting approach.[20] The anharmonic corrections to the vibrational frequencies were obtained by vibrational self-consistent-field (VSCF)[23,24] calculations at the RHF, MP2, CCSD and CCSD(T) levels by using the GAMESS[25] program. Dielectric effects of the solvent CH_2Cl_2 ($\varepsilon = 9.08$[26]) were estimated by using the COSMO conductor-like screening model.[27]

Experimental Section

General methods: All experiments were routinely carried out in an atmosphere of dry nitrogen. Solvents and glassware were dried and saturated/filled with nitrogen. Standard equipment was used throughout. Mass spectra were recorded on a Finnigan MAT 90 spectrometer by using FAB as an ionisation method. NMR spectra were obtained at room temperature in CD_2Cl_2 on JEOL-270. Chemical shifts are reported in δ values relative to the residual solvent resonances (^1H, ^{13}C). $^{31}P\{^1H\}$ NMR spectra are referenced to external aqueous H_3PO_4 (85%). The IR spectra were measured on a Perkin–Elmer FT-IR 577 spectrometer. (Me_3P)AuSCN was prepared by a published method.[28]

Thiocyanato-bis[(trimethylphosphine)gold] hexafluoroantimonate: (Me_3P)AuCl (93 mg, 0.30 mmol) was treated with $AgBF_4$ (103 mg, 0.32 mmol) in dichloromethane (15 mL) at −78 °C. The reaction mixture was stirred for 30 min and filtered into a precooled (−78 °C) solution of (Me_3P)AuSCN (100 mg, 0.30 mmol) in dichloromethane (10 mL). The reaction mixture was allowed to warm up slowly (2 h) to room temperature and stirred for another 3 h. The solvent was removed under reduced pressure and the collected residue was recrystallised from dichloromethane/*n*-pentane at −30 °C to give a colourless product (178 mg, 71%). M.p. 169 °C; ^1H NMR: $\delta = 1.67$ (d, $^2J(H,P) = 11.6$ Hz, Me); $^{13}C\{^1H\}$ NMR: $\delta = 15.7$ (d, $^1J(C,P) = 41.5$ Hz, Me); $^{31}P\{^1H\}$ NMR: $\delta = -7.3$ (s, PMe_3); IR (KBr): $\tilde{\nu} = 2161$ s, 2121 s, 2075 w ν(CN), 961 s ν(PC), 793 w ν(SC), 655 cm^{-1} vs ν(SbF); MS(FAB): *m/z*: 604.6 (100) $\{[(Me_3P)Au]_2SCN\}^+$, 349.5 (14.8) $[(Me_3P)_2Au]^+$, 332.4 (5.6) $[(Me_3P)AuSCN+H]^+$, 273.4 (74.4) $[(Me_3P)Au]^+$; elemental analysis calcd (%) for $C_7H_{18}Au_2F_6NP_2SSb$ (839.91 g mol^{-1}): C 10.01, H 2.16, N 1.67, S 3.82; found: C 10.32, H 2.18, N 1.75, S 3.71.

The absorption bands in the IR spectra (KBr pellets) of (Me_3P)AuSCN at 2113 and 2075 cm^{-1} were consistent with the work of Akhtar et al.[28] and could be assigned to the CN stretching vibration. A small band observed at 682 cm^{-1} (see Figure 1), which was not detected in the reference spectra of the starting material (Me_3P)AuCl, can be assigned to the SC stretching vibration. In other previously published IR data of complexes (R_3P)AuSCN (R = alkyl, aryl) this band was not detected due to overlapping of P–C bands in the same region.[1,29]

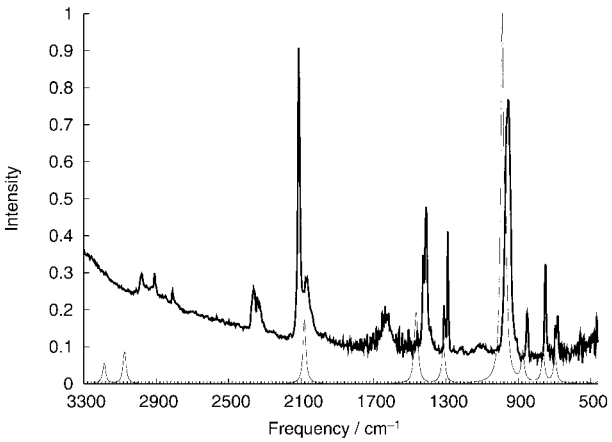

Figure 1. Harmonic frequencies calculated at the MP2/RDZ level compared with the experimental IR spectrum of (Me_3P)AuSCN (in KBr); calculated (——), measured (——).

Results

The thiocyanate anion: MP2 and CCSD(T) calculations on $[SCN]^-$ employing cc-pVDZ and cc-pVTZ basis sets show that the experimental bond lengths can be reproduced rather well at the MP2/cc-pVDZ level of theory. The largest deviation was obtained for the C–N bond which was found to be about 0.024 Å too long compared with the best literature value.[30] At the CCSD(T)/ccpVTZ level, the calculated bond lengths agree well with previously calculated values.[30] The CN stretching frequency, ν_{CN}, calculated at the

CCSD(T)/cc-pVTZ level, is in excellent agreement (within 2 cm^{-1}) with the experimental data, whereas the SC stretching frequency, ν_{SC}, calculated at the same level of theory is 33 cm^{-1} smaller than the experimental value. The results of the $[SCN]^-$ benchmark calculations are summarised in Table 1.

Table 1. Comparison of calculated and experimental structural parameters and vibrational frequencies of $[SCN]^-$. Harmonic vibrational frequencies and vibrational frequencies corrected for anharmonicity are listed. Bond lengths are given in Å, and frequencies in cm^{-1}.

			ν_{CN}		ν_{SC}	
	R_{S-C}	R_{C-N}	harm.	anharm.	harm.	anharm.
RHF/cc-pVDZ	1.691	1.152	2425	2399[a]	734	723[a]
RHF/cc-pVTZ	1.681	1.143	2397	2371[a]	739	728[a]
MP2/cc-pVDZ	1.676	1.203	2031	1995[a]	744	734[a]
MP2/cc-pVTZ	1.660	1.191	2018	1983[a]	748	739[a]
CCSD/cc-pVDZ	1.693	1.187	2175	–	720	–
CCSD/cc-pVTZ	1.678	1.172	2181	–	723	–
CCSD(T)/cc-pVTZ	1.677	1.181	2103	2068[b]	721	712[b]
CCSD(T)[30]	1.674	1.179	2091	2061[c]	720	708[c]
exptl[31,32]				2066[d]		745[e]

[a] VSCF calculation. [b] Extrapolated VSCF results, based on the MP2/cc-TZVP VSCF anharmonicity correction. [c] The rotational–vibrational energy levels were determined by a full 3D variational fitting of the energy surface.[30] [d] Measured in gas phase.[31] [e] Measured in a CsI matrix[32] and verified as a gas phase value by hot bands in the photo-electron spectrum.

The calculations on $[SCN]^-$ showed that high-quality wave-functions and large basis sets are needed to obtain accurate vibrational stretching frequencies. From Table 1, it is evident that anharmonic corrections must also be considered in order to obtain stretching frequencies in close agreement with experiment.

Although the MP2/cc-pVDZ calculations did not yield very accurate vibrational frequencies, the data seem to reflect the right trends. The accuracy of the calculated harmonic and anharmonic contributions to the vibrational frequencies is sufficient to generate an extrapolation scheme based on a combination of experimental data and computational results. The IR data obtained using this extrapolation procedure are very useful for a verification of the molecular structures proposed in this study.

The bis[(phosphine)gold(I)]chloronium cation: The $[(H_3PAu)_2Cl]^+$ cation, displayed in Figure 2, was used to probe the capability of the computational methods to describe the gold–gold interactions correctly. The Au–Au distance of 4.190 Å obtained at the RHF level is 0.97 Å longer than the experimental value of 3.22 Å for $[(Ph_3PAu)_2Cl]ClO_4{\cdot}CH_2Cl_2$.[10] This is as expected, since the aurophilic attraction is predominantly a dispersion interaction, which is considered only in correlation calculations.[12]

The difference of 0.58 Å between the Au–Au distances calculated at the MP2/DZ and MP2/RDZ levels is surprisingly large and shows the significance of the polarisation f functions on Au for a correct description of the aurophilic attraction.[16] This has also been demonstrated in earlier studies.[12,33] The Au–Au distance of 3.181 Å obtained at the MP2/RDZ level is in excellent agreement with the experimental value of 3.22 Å. Since MP2/RDZ calculations can be applied on all molecular species of this study, and all geometrical parameters for $[(Ph_3PAu)_2Cl]ClO_4{\cdot}CH_2Cl_2$ calculated at this level are in good agreement with those measured in the solid state,[10] the MP2/RDZ calculations are adopted here as the main computational level. The results of the benchmark calculations on $[(H_3PAu)_2Cl]^+$ are given in Table 2.

It is to be expected that for ion pairs or in the condensed phase there will be a significant influence of the counterions. This effect is likely to reduce the attraction between the cations as recently demonstrated for other systems.[34]

Isomeric mononuclear gold(I) thiocyanate complexes $(R_3P)AuSCN$: For a realistic verification of the accuracy of the MP2/RDZ results, calculations at this level of theory were performed on mononuclear gold(I) thiocyanate complexes such as the hypothetical $(H_3P)AuSCN$ and the known $(Me_3P)AuSCN$. These molecules are good reference compounds for this purpose, since

Table 2. Comparison of calculated (R = H) and experimental (R = Ph) values for some structural parameters of $[(R_3PAu)_2Cl]^+$. Bond lengths are given in Å and angles in degrees.

	Calculated			Xrd.[a]
	RHF/RDZ	MP2/DZ	MP2/RDZ	
R_{Au-Cl}	2.438	2.401	2.345	2.328–2.345
R_{Au-Au}	4.190	3.763	3.181	3.22
$\alpha_{Au-Cl-Au}$	118.5	103.2	85.4	92

[a] X-ray data for $[(Ph_3PAu)_2Cl]^+$.[10]

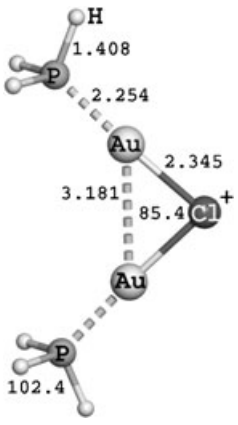

Figure 2. Equilibrium structures of the bis[(phosphine)gold(I)]chloronium cation calculated at the MP2/RDZ level. The distances are given in Å and the angles in degrees.

accurate experimental data are available not only for $(Me_3P)AuSCN$, but also for several homologues with larger tertiary phosphines.[1,35] $(Me_3P)AuSCN$ forms a tetramer in the solid state with a rather short intermolecular Au–S distance of 3.771(2) Å. The formation of a tetramer may influence the electronic and the molecular structure in this particular case but all other complexes are monomeric in the solid state. The heteroleptic form $(Me_3P)AuSCN$, with more than one type of ligand at the transition metal, is just one possible isomer of the net composition $(R_3P)AuSCN$ (see Figure 3).

The heavy atom skeleton of $(H_3P)AuSCN$ as calculated at the MP2/RDZ level agrees well with the framework of the X-ray structures of $(Me_3P)AuSCN$ and $[(o\text{-tol})_3P]AuSCN$. The comparison of the molecular structures of $(H_3P)AuSCN$ and $(Me_3P)AuSCN$ in Table 3 shows that it is justified to use PH_3 as a model for PMe_3 in the calculation of geometrical parameters and vibrational frequencies. This is a common approximation in computational gold chemistry.[12]

At the MP2/RDZ level, the largest difference between the structures of $(H_3P)AuSCN$ and $(Me_3P)AuSCN$ is found for the Au–P distance (2.306/2.247 Å). This can be rationalised as a consequence of the slightly enhanced electron donating effect (+I effect) and hyperconjugation (−M effect) of the methyl groups compared to hydrogen, resulting in a shorter and stronger bonding of the ligand in $(Me_3P)AuSCN$. This effect propagates to a small extent to the $Au^{\delta+}-S^{\delta-}$ bond, which is found to be somewhat longer in $(H_3P)AuSCN$ than in $(Me_3P)AuSCN$. At the MP2/RDZ level, the Au–S distances obtained for $(H_3P)AuSCN$ and $(Me_3P)AuSCN$ are 2.308 and 2.295 Å, respectively.

The harmonic C–N and C–S stretching frequencies of 2087 and 2081 cm^{-1} and of 700 and 701 cm^{-1} calculated at the MP2/RDZ level for $(H_3P)AuSCN$ and $(Me_3P)AuSCN$, respectively, are in good agreement with experimental IR data, $\nu_{CN}=2113$ and $\nu_{CS}=682$ cm^{-1} for $(Me_3P)AuSCN$.[28]

In solution, the heteroleptic form $(R_3P)AuSCN$ may be the component of an equilibrium including the two homoleptic ionic species as demonstrated, for example, for cyano gold(I) complexes[29,36–38] or anions X^- other than thiocyanate.[1,28,39–42] The ionic form may also appear in the solid state [Eq. (2)].

A second heteroleptic form to be considered is the N-bonded isomer, which can also be involved in such equilibria [Eq. (3)]:

$$2\,(R_3P)AuSCN \rightleftharpoons [(R_3P)_2Au]^+ + [Au(SCN)_2]^- \quad (2)$$

$$(R_3P)AuSCN \rightleftharpoons (R_3P)AuNCS \quad (3)$$

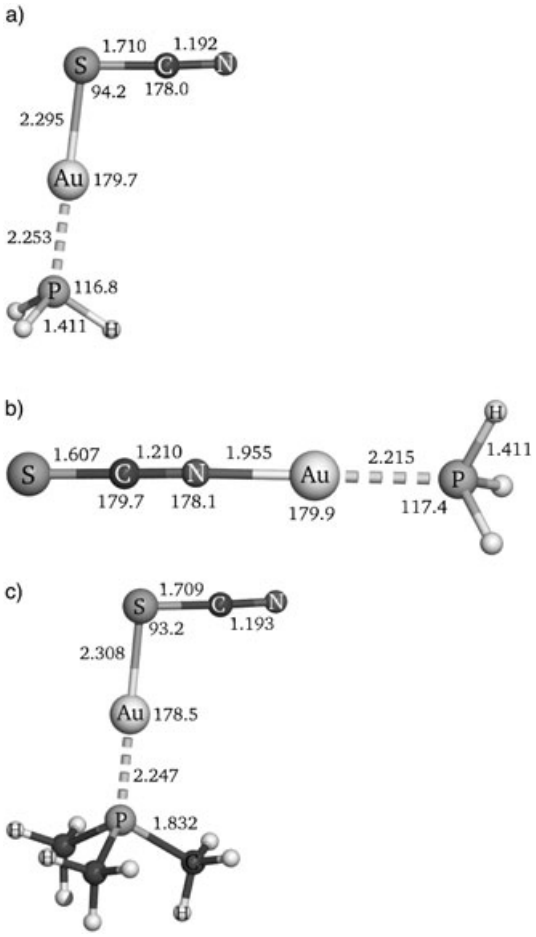

Figure 3. Equilibrium structures of the monoaurated thiocyanate anions calculated at the MP2/RDZ level: a) $(H_3P)AuSCN$ (0.0 kcal mol^{-1}), b) $(H_3P)AuNCS$ (2.0 kcal mol^{-1}), c) $(Me_3P)AuSCN$. The distances are given in Å, the angles in degrees; the calculated (MP2/RDZ/COSMO) relative energies are given in parentheses.

Table 3. Structural parameters and vibrational frequencies of $(R_3P)AuSCN$ complexes calculated at the RHF/RDZ and MP2/RDZ levels as compared to experimental data. Bond lengths are given in Å, angles in degrees and frequencies in cm^{-1}.

	Calculated				Xrd.	
R→	H		Me		Me[a]	*o*-tol[b]
	RHF	MP2	RHF	MP2	tetramer	monomer
R_{N-C}	1.141	1.192	1.142	1.193	1.167(14)	1.147(4)
R_{C-S}	1.712	1.710	1.712	1.709	1.673(11)	1.681(3)
R_{Au-S}	2.381	2.295	2.393	2.308	2.334(2)	2.3256(8)
R_{Au-P}	2.360	2.306	2.356	2.247	2.252(2)	2.2726(7)
α_{N-C-S}	179.1	178.8	179.5	178.5	175.6(1)	177.1(3)
α_{C-S-Au}	98.3	94.2	97.9	93.2	102.7(3)	98.75(11)
ν_{CN}	2516	2087	2511	2081	2113[c]	2120[c]
ν_{CS}	722	700	721	701	682[c]	–[d]

[a] X-ray data from ref. [35]. [b] X-ray data from ref. [1]. [c] IR spectra (KBr). [d] Not observed due to overlapping P–C modes.

Equilibria of type (3) have been frequently observed and studied with other metal atoms[28,39–42] and are quite well understood at an empirical level in terms of the so called *antisymbiotic* trans effect predominantly at class (b) metals.[41–43] To our knowledge, N-bonded gold(I) thiocyanate complexes

have not previously been reported.

The first step in the present computational study of Equilibrium (3) was to calculate the structures of the $(H_3P)AuSCN$ and $(H_3P)AuNCS$ isomers. At the MP2/RDZ level, local minima were obtained on the potential-energy surface for both molecular isomers with ground-state molecular structures shown in Figure 3 and geometrical parameters given in Tables 3 and 4. Results for S-bonded $(H_3P)AuSCN$ and $(Me_3P)AuSCN$ were discussed in the previous Section.

Table 4. Structural parameters and vibrational frequencies of $(H_3P)AuNCS$ calculated at the RHF/RDZ and MP2/RDZ levels. Bond lengths are given in Å, angles in degrees, and frequencies in cm^{-1}.

	RHF	MP2
R_{S-C}	1.628	1.607
R_{C-N}	1.159	1.210
R_{N-Au}	2.029	1.955
R_{Au-P}	2.312	2.215
R_{H-P}	1.404	1.411
α_{S-C-N}	180.0	179.7
α_{C-N-Au}	178.4	178.1
α_{N-Au-P}	179.8	179.9
α_{Au-P-H}	117.1	117.4
ν_{CN}	2349	2075
ν_{CS}	901	748

At the MP2/RDZ level, the optimisation of the molecular structure of the $(H_3P)AuNCS$ isomer yielded equilibrium structures with exclusively real vibrational frequencies. The main structural difference between the N-bonded and the S-bonded complex is the angle at the donor atom (N/S): For $(H_3P)AuSCN$, the Au-S-C angle is 97.9° (MP2/RDZ) that is, slightly larger than a right angle, whereas $(H_3P)AuNCS$ has colinear Au–N and N–C bonds; the Au-N-C angle is 180°. The Au–N distance of 1.955 Å (MP2/RDZ) is rather short. Thus, in terms of Lewis formulae, the mesomeric form A in Equation (4) seems to be slightly more significant than for the S-bonded complex. A dominating B character would imply an sp^2 hybridisation and consequently a C-N-Au angle of about 120°, which is for example, observed in the solid state structure of the $[Cu^{II}(NCS)(tim)]PF_6$ complex.[44]

At the MP2/RDZ level, the C–N bond in $(H_3P)AuNCS$ is 1.210 Å compared with 1.192 Å in $(H_3P)AuSCN$, whereas the C–S bond is longer in $(H_3P)AuSCN$ (1.607/1.710 Å for $(H_3P)AuNCS/(H_3P)AuSCN$).

Gold is known to be a distinctly thiophilic metal, which suggests a significant energy difference between the S-bonded and the N-bonded isomers, favouring the S-bonded form. Surprisingly, the energy release of the isomerisation reaction (ΔE_{iso}) in Equation (5), with R = H, is calculated at the MP2/RDZ level to be only $-3.6\,kcal\,mol^{-1}$. See Table 5.

$$^{\ominus}|\overline{S}-C\equiv N| \;\leftrightarrow\; \overline{S}=C=\overline{N}^{\ominus} \qquad (4)$$

A B

$$(R_3P)AuNCS \rightleftharpoons (R_3P)AuSCN \qquad (5)$$

Table 5. Isomerisation energy (ΔE_{iso} in $kcal\,mol^{-1}$) and the frequencies (in cm^{-1}) for the C–N stretching vibration of $(R_3P)AuNCS$ and $(R_3P)AuSCN$ (with R = H) calculated at the RHF/RDZ and MP2/RDZ levels as compared to experimental data (for R = Me).

	Calculation			Exptl[a]
	RHF	MP2	MP2[b]	IR
ΔE_{iso}	−2.2	−3.6	−2.0	−4.2
$\nu_{CN}(\{R_3P\}AuNCS)$	2349	2075	–	2075
$\nu_{CN}(\{R_3P\}AuSCN)$	2516	2087	–	2113

[a] Obtained using $\Delta E_{iso} = -RT\ln k$ at 298 K and k from integrated and calculated IR intensities (MP2/RDZ). [b] Dielectrical continuum effect of CH_2Cl_2 were considered by using the COSMO model.

This value can be compared to an estimated free energy ΔG of $-4.2\,kcal\,mol^{-1}$ for the Equilibrium (5) with R = Me, deduced from the IR spectrum measured in CH_2Cl_2 solution. Assuming a linear relation between concentrations and IR intensities, the equilibrium constant, k, and the free energy, ΔG, can be obtained from the ratio of the integrated intensities of a certain vibrational mode of the different species. The intensities obtained have to be scaled with the calculated ratios of the same modes. The integration of the two ν_{CN} peaks at 2113 and $2075\,cm^{-1}$ in the spectrum of $(Me_3P)AuSCN$ shown in Figures 1 and 5 yields a ratio of 15:1. At the MP2/RDZ level, the intensities of $\nu_{CN}(\{H_3P\}AuSCN)$ and $\nu_{CN}(\{H_3P\}AuNCS)$ are 0.46 and $41.90\,km\,mol^{-1}$, respectively. This yields an equilibrium constant k of $1.366\cdot10^3$ and a ΔG value of $-4.2\,kcal\,mol^{-1}$, which is in good agreement with the ΔE_{iso} values given in Table 5 calculated for the gas phase. The equilibrium constant of 1.1 reported by Akhtar et al. differs from this value since it is obtained using an estimated IR absorption ratio of 1:10.[28]

Estimates for ΔG, ΔH and ΔS in the gas phase can be obtained by also considering the vibrational energy contributions. The obtained values for ΔG and ΔH differ by less than $1.0\,kcal\,mol^{-1}$ from ΔE_{iso}, since the entropy (ΔS) calculated at the MP2/RDZ level is only $0.1\,cal\,mol^{-1}\,K^{-1}$.

The vibrational frequency calculations on $[SCN]^-$ revealed difficulties to accurately reproduce experimental IR spectra. However, the computational errors for the vibrational frequencies of the thiocyanate complex are expected to be cancelled to a large extent by employing an extrapolation scheme with the vibrational frequencies of $[SCN]^-$ as reference. Thus, improved values for the C–N and S–C stretching vibrations (Y) of the thiocyanate complex (X) can be obtained as given in Equation (6):

$$\nu_Y^{est}(X) = \nu_Y^{calcd}(X) + \{\nu_Y^{exptl}([SCN]^-) - \nu_Y^{calcd}([SCN]^-)\} \qquad (6)$$

where $\nu_Y^{calcd}(X)$ is the calculated stretching frequency of the

thiocyanate complex, $\nu_Y^{calcd}([SCN]^-)$ the corresponding calculated IR frequency of $[SCN]^-$, $\nu_Y^{exptl}([SCN]^-)$ its experimental IR frequency, and $\nu_Y^{est}(X)$ the extrapolated IR frequency for the thiocyanate complex. The vibrational frequencies and the corresponding vibrational frequency shifts are listed in Table 6. The extrapolated values for those vibrational modes which $[SCN]^-$ and the thiocyanate complex have in common are to some extent corrected for anharmonicities, solvent effects, and computational uncertainties. The extrapolated value for $\nu_Y^{est}(\{H_3P\}AuSCN)$ is 2122 cm^{-1}, whereas the corresponding band in the IR spectrum of $(Me_3P)AuSCN$ appears at 2113 cm^{-1} (see Table 7).

Table 6. Vibrational frequencies [$\nu_{CN}(X)$, $\nu_{CS}(X)$ in cm^{-1}] and vibrational frequency shifts [$\Delta\nu_Y(X) = \nu_Y(X) - \nu_Y([SCN]^-)$ in cm^{-1}] for the thiocyanates calculated at the MP2/RDZ level compared with the experimental values.

	$\nu_{CN}(X)$		$\Delta\nu_{CN}(X)$		$\nu_{CS}(X)$		$\Delta\nu_{CS}(X)$	
R→	H	Me	H	Me	H	Me	H	Me
X	Calcd	Exptl	Calcd	Exptl	Calcd	Exptl	Calcd	Exptl
$[SCN]^-$	2031	2066[a]	0	0	748	745[b]	0	0
$(R_3P)AuNCS$	2075	2075	44	9	971	–[c]	223	–
$(R_3P)AuSCN$	2087	2113	56	47	700	682	−48	−63
$[(R_3PAu)_2NCS]^+$	1917	–[d]	−114	–	960	–[c]	212	–
$[(R_3PAu)_2SCN]^+$	2089	2121	58	55	680	–[e]	−68	–
$[(R_3P)AuSCNAu(PR_3)]^+$	2140	2161	109	95	819	793	71	48

[a] Measured for $[SCN]^-$ in gas phase.[31] [b] Measured for $[SCN]^-$ in a CsI matrix[32] and verified as a gas phase value by hot bands in the photo-electron spectrum. [c] The band was obscured by the strong absorptions of P–C modes of the PMe_3 group. [d] This band was not observed. [e] The band was obscured by the strong $[SbF_6]^-$ absorptions.

Table 7. Extrapolated frequencies (in cm^{-1}) for the C–N and C–S stretching vibrations of thiocyanates obtained by using Equation (6) compared with available experimental values. The extrapolated values are deduced from MP2/RDZ data.

	$\nu_{CN}^{exptl[a]}$	$\nu_{CN}^{est[b]}$	$\nu_{CS}^{exptl[a]}$	$\nu_{CS}^{est[b]}$
$[SCN]^-$	2066[c]	(2066)	745[d]	(745)
$(R_3P)AuNCS$	2075	2110	–[e]	969
$(R_3P)AuSCN$	2113	2122	682	698
$[(R_3PAu)_2NCS]^+$	–[f]	1952	–[e]	957
$[(R_3PAu)_2SCN]^+$	2121	2124	–[g]	678
$[(R_3PAu)SCN(AuPR_3)]^+$	2161	2175	793	816

[a] R = Me. [b] R = H. [c] Measured in gas phase.[31] [d] Measured in a CsI matrix[32] and verified as a gas phase value from hot bands in the photoelectron spectrum. [e] The band was obscured by the strong absorptions of P–C modes of the PMe_3 group. [f] This band was not observed. [g] The band was obscured by the strong $[SbF_6]^-$ absorptions.

These values can be further improved by also considering differences in the anharmonic corrections $[^{ah}\nu_Y(X)]$ in a similar manner

$$^{ah}\nu_Y^{est}(X) = \nu_Y^{est}(X) + \{^{ah}\nu_Y^{calcd}([SCN]^-) - \nu_Y^{calcd}([SCN]^-)\} \quad (7)$$

Anharmonic corrected frequencies for $(H_3P)AuSCN$ and $(H_3P)AuNCS$ were estimated by using this procedure. The anharmonic corrections for $[SCN]^-$ were calculated by using the VSCF approach[24] as implemented in GAMESS[23] (see Table 1). The extrapolated vibrational frequencies including anharmonic corrections are 2086 and 2074 cm^{-1} for $^{ah}\nu_{CN}^{est}(\{H_3P\}AuSCN)$ and $^{ah}\nu_{CN}^{est}(\{H_3P\}AuNCS)$, respectively. These values are in reasonable agreement with the corresponding experimental values of 2113 and 2075 cm^{-1}, respectively.

The results of these analyses for the vibrational frequencies of $(H_3P)AuNCS$ and $(H_3P)AuSCN$ are consistent with conclusions by Akhtar et al.,[28] who assigned the prominent IR band at 2113 cm^{-1} to $(Me_3P)AuSCN$ and the weaker band at 2075 cm^{-1} to $Me_3PAuNCS$.

Isomeric dinuclear gold(I) thiocyanate complexes $\{[(R_3P)Au]_2(SCN)\}^+X^-$: Digold(I) thiocyanate complexes can be synthesised by adding one equivalent of $[(R_3P)Au]^+X^-$ to Equilibrium (3). At least three isomers can be proposed which are compounds of a new equilibrium:

$$\{[(R_3P)Au]_2SCN\}^+ \rightleftharpoons \{[(R_3P)Au]SCN[Au(PR_3)]\}^+ \rightleftharpoons \{[(R_3P)Au]_2NCS\}^+ \quad (8)$$

with the energetically lowest isomer dominating.

The geometry optimisations at the MP2/RDZ level for the cation with R = H yielded local minima for each of the three isomers, with $[(H_3PAu)SCN(AuPH_3)]^+$ as the most stable species, followed by $[(H_3PAu)_2NCS]^+$. The energy difference between these isomers is 7.9 kcal mol^{-1}, while $[(H_3PAu)_2SCN]^+$ lies 10.6 kcal mol^{-1} above $[(H_3PAu)SCN(AuPH_3)]^+$. The data calculated for the three isomers are summarised in Table 8, and the structures are shown in Figure 4.

In the gas phase, the $[(H_3PAu)SCN(AuPH_3)]^+$ species (see Figure 4b) has the structural features of both the $(H_3P)AuSCN$ and the $(H_3P)AuNCS$ molecule. The Au–N/Au–S bonds appear to be weaker than in the reference molecule, since the distances are slightly larger and the Au-S-C bond angle is wider: At the MP2/RDZ level, the N–Au distance in $[(H_3PAu)SCN(AuPH_3)]^+$ is 2.054 compared with 1.955 Å for $(H_3P)AuNCS$. Similarly, the S–Au distance in the former is 2.391 and 2.295 Å for $(H_3P)AuSCN$. The Au-S-C angle in $[(H_3PAu)SCN(AuPH_3)]^+$ is 98.4 compared with 94.2° for $H_3PAuSCN$.

For $[(H_3PAu)_2SCN]^+$ with C_s symmetry (see Figure 4a), the trends observed in the structural changes from $[SCN]^-$ via $(H_3P)AuSCN$ to $[(H_3PAu)_2SCN]^+$ continue: At the MP2/

Table 8. Gold–gold distances [R(Au–Au) in Å] of the three isomeric diaurated thiocyanate cations (with R = H) calculated at the RHF and MP2 levels by using the DZ and RDZ basis sets. The isomerisation energies (ΔE_{iso} in kcal mol^{-1}) relative to $[(R_3PAu)SCN(AuPR_3)]^+$ calculated at different levels are also given.

	R(Au–Au)			ΔE_{iso}				
	RHF[b]	MP2[a]	MP2[b]	RHF[b]	MP2[a]	MP2[b]	MP2[c]	Exptl[d]
$[(R_3PAu)SCN(AuPR_3)]^+$	6.122	5.921	5.839	0	0	0	0	–
$[(R_3PAu)_2NCS]^+$	3.778	3.609	3.414	+9.5	+8.7	+7.9	+7.2	–
$[(R_3PAu)_2SCN]^+$	4.165	3.740	3.208	+14.0	+13.9	+10.6	−1.2	≈2.0

[a] The DZ basis set was used. [b] The RDZ basis set was used. [c] Dielectrical continuum effects of CH_2Cl_2 were considered by using the COSMO model. [d] This is an estimate for the R = Me compound based on the IR intensity integrals and the MP2/RDZ level IR intensities.

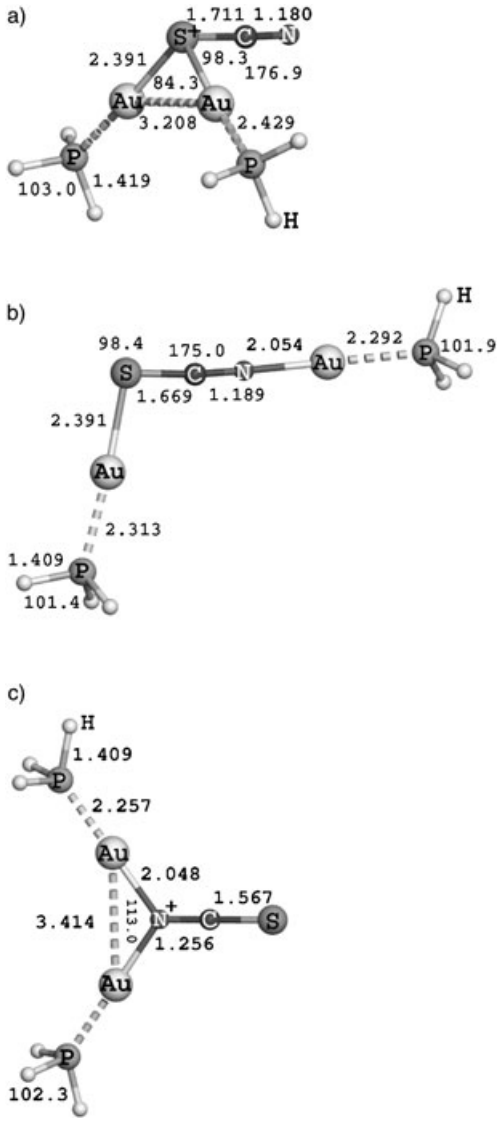

Figure 4. Equilibrium structures of three isomeric digold(I) thiocyanate cations calculated at the MP2/RDZ level: a) $\{(H_3PAu)_2SCN\}^+$ (0.0 kcal mol^{-1}), b) $\{(H_3PAuSCNAuPH_3\}^+$ (1.2 kcal mol^{-1}), c) $\{(H_3PAu)_2NCS\}^+$ (8.4 kcal mol^{-1}) The distances are given in Å, the angles in degrees; the calculated (MP2/RDZ/COSMO) relative energies are given in parentheses.

RDZ level, the C–N distance decreases in $[SCN]^-$ from 1.203 to 1.192 and 1.118 Å whereas the S–C distance increases systematically from 1.676 to 1.710 to 1.711 Å for $[SCN]^-$, $(H_3P)AuSCN$, and $[(H_3PAu)_2SCN]^+$, respectively. For $[(H_3PAu)_2SCN]^+$, the two Au–S bonds of 2.391 Å are 0.1 Å longer than for the S-monoaurated and S,N-diaurated species.

The Au-S-C angles are 98.3° in $[(H_3PAu)_2SCN]^+$ and 98.4° in the $[(H_3PAu)SCN(AuPH_3)]^+$ cation. The small Au-S-Au angle of 84.3° in the former leads to a short aurophilic contact of 3.208 Å. This distance is slightly larger than in the reference cation $[(R_3PAu)_2Cl]^+$ which has an Au–Au distance of 3.181 Å calculated at MP2/RDZ level with R = H. For comparison, the experimental Au–Au distance in the solid state structure of $[(Ph_3PAu)_2Cl]^+$ is 3.22 Å.[10]

The strength of the intramolecular Au–Au interaction in $[(H_3PAu)_2SCN]^+$ is estimated at the MP2/RDZ level to 3.5–3.6 kcal mol^{-1}. This value is obtained from a comparison of the energies for the isomerisation Reaction (9):

$$[(H_3PAu)_2SCN]^+ \rightarrow [(H_3PAu)SCN(AuPH_3)]^+;\ \Delta E_{iso} \qquad (9)$$

At the MP2/DZ level, that is, without f functions for the Au atoms, one obtains a ΔE_{iso}, value of −13.9 kcal mol^{-1}. The addition of f functions for gold stabilises the μ^2-S isomer with direct Au–Au interactions resulting in a lower isomerisation energy of −10.6 kcal mol^{-1}. The energy difference of 3.5 kcal mol^{-1} between the isomerisation energies calculated at the MP2/RDZ and MP2/DZ levels is an estimate of the intramolecular aurophilic attraction energy for this species. The use of a larger basis set would yield a stronger aurophilic interaction. However, since MP2 tends to overestimate Au−Au bond strengths,[45] the MP2/RDZ calculations seems to describe the aurophilic interaction rather well. See Table 2. The obtained isomerisation energies are summarised in Table 8.

The μ^2-N isomer $[(H_3PAu)_2NCS]^+$ with C_{2v} symmetry shown in Figure 4c was found at the MP2/RDZ level to be 2.7 kcal mol^{-1} lower in energy than the μ^2-S isomer $[(H_3PAu)_2SCN]^+$. This is a remarkable result which is not in agreement with the generally accepted idea of a pronounced thiophilic nature of Au^+.[12] This thiophilic nature has also been confirmed here by the calculations on the monoaurated thiocyanate isomers. Contrary to the μ^2-S isomer, the μ^2-N isomer with its distorted-trigonal-planar configuration of the nitrogen atom has a planar heavy atom skeleton. The Au–N distance of 2.048 Å is almost the same as for the monoaurated species. The Au-N-C angles of 123.5° are very close to the sp^2 angle of 120°. The Au–Au distance in the μ^2-N isomer of 3.414 Å (MP2/RDZ) is large and indicates very weak intramolecular aurophilic interactions of 0.8–1.6 kcal mol^{-1}, estimated from the isomerisation energies for Reactions (9) and (10) given in Table 8.

$$[(H_3PAu)_2NCS]^+ \rightleftharpoons [(H_3PAu)NCS(AuPH_3)]^+ \quad (10)$$

For the interpretation of the experimental IR spectrum of the diauration products, frequency analyses at the MP2/RDZ level by using the same extrapolation procedure as described above were carried out. The calculated frequencies for the C–N stretching vibration (ν_{CN}) are 2140, 2089 and 1917 cm^{-1} for the cations $[(H_3PAu)SCN(AuPH_3)]^+$, $[(H_3PAu)_2SCN]^+$ and $[(H_3PAu)_2NCS]^+$, respectively (see Table 6). The extrapolation procedure yields estimated values (ν_{CN}^{est}) of 2175, 2124 and 1952 cm^{-1}, see Table 7. These are in very good agreement with the frequencies of the two IR bands at 2161 (strong, broad) and 2121 cm^{-1} (weak, sharp) obtained for the corresponding Me_3P complex(es) (see Table 7 and Figure 5). The IR spectrum was recorded for the reaction product of the diauration Reaction (1) (with R = Me). The band predicted at 1952 cm^{-1} was not observed.

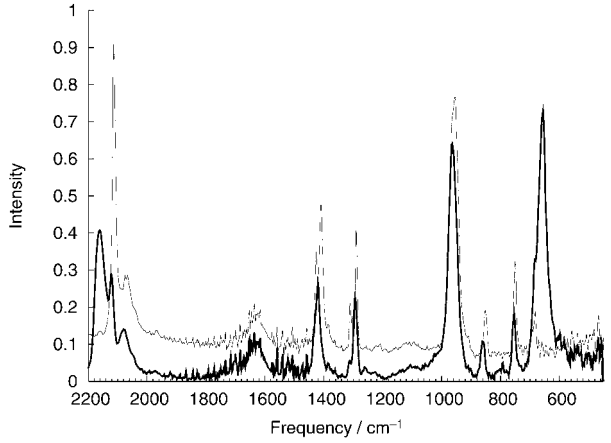

Figure 5. Comparison of the experimental IR spectra of $Me_3PAuSCN$ (——) and $[(Me_3PAu)_2SCN]^+[SbF_6]^-$ (——) measured in KBr.

The C–S stretching vibrations were also calculated. Due to P–C vibrations and other IR modes which also appear in the finger-print region, only the peak at 793 cm^{-1} can be assigned to ν_{SC} of the $[(H_3PAu)SCN(AuPH_3)]^+$ cation. The MP2/RDZ and extrapolated values are 819 and 816 cm^{-1}, respectively (see also Tables 6 and 7).

The calculated relative energies of the three isomers can be compared with measured IR intensities using the same procedure as previously applied for the two monoauration isomers. Only two ν_{CN} signals of the diauration products can be assigned to different diauration isomers obtained in Reaction (1). The ratio of these integrated intensities for $\nu\{[(H_3PAu)SCN(AuPH_3)]^+\}$:$\nu\{[(H_3PAu)_2SCN]^+\}$ of the measured IR spectrum is 9:1, while the ratio of the corresponding calculated IR intensities (MP2/RDZ) is 270:1, yielding an equilibrium constant k of 30. This k value corresponds to a free energy of +2.0 kcal mol^{-1} for Reaction (9).

The calculated vibrational frequencies confirm the proposed structures of the cations in equilibrium, whereas the calculated relative energies seem to contradict the observed IR intensities. However, by also considering effects from the dielectric continuum in the computational model the calculated isomerisation energies for Reaction (9) change sign. A significant stabilisation by −10.4 kcal mol^{-1} of the μ^2-S isomer relative to the μ^1-N–μ^1-S isomer was found. This is in contrast to the monoauration isomers, where only small matrix effects where found. Also for the μ^2-N isomer only a minor stabilisation of −1.7 kcal mol^{-1} was obtained. The stabilization energy obtained in the COSMO calculation is roughly proportional to the size of the molecular dipole moment. According to the population analysis, the thiocyanate in the μ^2-S isomer has a significantly larger charge separation than for the two other isomers explaining the large solvent stabilization energy for the μ^2-S isomer.

This makes the $[(H_3PAu)_2SCN]^+$ cation the most stable isomer, followed by the $[(H_3PAu)SCN(AuPH_3)]^+$ cation which is 1.2 kcal mol^{-1} higher in energy and then followed by the $[(H_3PAu)_2NCS]^+$ cation, which lies 8.4 kcal mol^{-1} above the $[(H_3PAu)_2SCN]^+$ cation. These isomerisation energies were obtained at the MP2/RDZ level including the dielectric continuum corrections.

Conclusion

The isomeric mononuclear gold(I) thiocyanate model compounds, $(H_3P)AuSCN$ and $(H_3P)AuNCS$, were found to represent minima on the potential energy surface. The molecular structure of the S-bonded compound calculated at the MP2/RDZ level agrees well with the X-ray structures of $(Me_3P)AuSCN$ and $\{(o\text{-tol})_3P\}AuSCN$. Substitution of H_3P by Me_3P had no significant influence on the structure, vibrational frequencies, and the relative energies of the two complexes, that is, the isomerisation energy. The calculations yielded an unambiguous assignment of the C–N stretching vibrations observed in the IR spectrum. The IR peaks observed at 2113 and 2075 cm^{-1} correspond to $\nu_{CN}^{exptl}(\{Me_3P\}AuSCN)$ and $\nu_{CN}^{exptl}(\{Me_3P\}AuNCS)$, respectively. Even though gold is a thiophilic metal suggesting a significantly lower energy for the S-bonded ($\{H_3P\}AuSCN$) isomer than for the N-bonded one ($\{H_3P\}AuNCS$), the MP2/RDZ calculations including a solvent energy shift of 1.6 kcal mol^{-1} indicated that the S-bonded isomer lies only 2.0 kcal mol^{-1} below $(H_3P)AuNCS$. An experimental isomerisation energy of 4.0 kcal mol^{-1} can be deduced from the ratio between the intensities of the $\nu_{CN}^{exptl}(\{Me_3P\}AuSCN)$ and $\nu_{CN}^{exptl}(\{Me_3P\}AuNCS)$ scaled by the calculated ratio of the absorption coefficients of the two IR peaks; both computationally and experimentally the S-bonded isomer is found to lie only a few kcal mol^{-1} below the N-bonded isomer.

The three dinuclear gold(I) thiocyanate complexes $[(H_3PAu)_2SCN]^+$, $[(H_3PAu)_2NCS]^+$ and $[(H_3PAu)SCN(AuPH_3)]^+$ considered were all found to represent distinct minima on the potential energy surface. The two geminally substituted S-bonded (μ^2-S) or N-bonded (μ^2-N) complexes form Au–Au contacts of approximately 3.21 and 3.41 Å, as-

sociated with an intramolecular aurophilic stabilisation energies of about 4 and 1 kcal mol^{-1}, respectively. The aurophilic interaction energies obtained fit well in the area defined for such interactions given in Figure 10 of ref. [12]. The doubly substituted S- and N-bonded complex (μ^1-S–μ^1-N) is not stabilised by any aurophilic interaction.

The C–N stretching vibrations of the dinuclear complexes were calculated with high accuracy and the corresponding vibration modes observed in the IR could be unambiguously assigned. The C–N stretching mode ($\nu_{CN}^{exptl}([(H_3PAu)_2SCN]^+$) of the μ^2-S complex appears at 2121 cm^{-1} and the C–N stretching frequency of the μ^1-S–μ^1-N complex (ν_{CN}^{exptl} $[(H_3PAu)SCN(AuPH_3)]^+$) is 2161 cm^{-1} compared with the corresponding calculated values of 2124 and 2175 cm^{-1}, respectively. So far, no evidence for the μ^2-N complex has been found in measured IR spectra. According to the present calculations, the peak of the C–N stretching mode for the μ^2-N complex should show up at about 1950 cm^{-1}. The MP2/RDZ calculations including dielectrical continuum effects of CH_2Cl_2 suggest that the $[(H_3PAu)_2SCN]^+$ isomer lies energetically lowest, followed by $[(H_3PAu)SCN(AuPH_3)]^+$ and $[(H_3PAu)_2NCS]^+$ which are 1.2 and 8.4 kcal mol^{-1} higher in energy, respectively. This stability order is also supported by a comparison of calculated and measured IR intensities.

Acknowledgements

We acknowledge the support from the European research training network on "Molecular Properties and Molecular Materials" (MOLPROP), contract No. HPRN-2000-00013, and The Academy of Finland grants 53915, 173235 and 200903. We also thank Prof. R. Ahlrichs for a copy of Turbomole.

[1] D. Schneider, S. Nogai, A. Schier, H. Schmidbaur, *Inorg. Chim. Acta* **2003**, *352*, 179.
[2] H. G. Raubenheimer, S. Cronje in *Gold, Progress in Chemistry, Biochemistry and* Technology (Ed.: H. Schmidbaur), Wiley, Chichester, **1999**, pp. 557.
[3] M. D. Adams, M. W. Jones, D. W. Dew in *Gold, Progress in Chemistry, Biochemistry and* Technology (Ed.: H. Schmidbaur), Wiley, Chichester, **1999**, pp. 65.
[4] H. Grossmann, K. E. Saenger, E. Vinaricky, in *Gold, Progress in Chemistry, Biochemistry and* Technology (Ed.: H. Schmidbaur), Wiley, Chichester, **1999**, pp. 199.
[5] R. J. Puddephatt in *Gold, Progress in Chemistry, Biochemistry and* Technology (Ed.: H. Schmidbaur), Wiley, Chichester, **1999**, pp. 237.
[6] *Gmelin Handbook of Inorganic Chemistry, Gold, Supplement, Volume B1*, Springer, Berlin, **1992**.
[7] *Gmelin Handbook of Inorganic Chemistry, Gold, Supplement, Volume B2*, Springer, Berlin, **1994**.
[8] H. Schmidbaur, A. Hamel, N. W. Mitzel, A. Schier, S. Nogai, *Proc. Natl. Acad. Sci. USA* **2002**, *99*, 4919.
[9] A. Bayler, A. Bauer, H. Schmidbaur, *Chem. Ber.* **1997**, *130*, 115.
[10] P. G. Jones, G. M. Sheldrick, R. Uson, A. Laguna, *Acta. Crystallogr. Sect. B* **1980**, *36*, 1486.
[11] P. Schwerdtfeger, P. D. W. Boyd, A. K. Burrell, W. T. Robinson, M. J. Taylor, *Inorg. Chem.* **1990**, *29*, 3593.
[12] P. Pyykkö, *Chem. Rev.* **1997**, *97*, 597.
[13] T. H. Dunning Jr, *J. Chem. Phys.* **1989**, *90*, 1007.
[14] D. E. Woon, T. H. Dunning Jr, *J. Chem. Phys.* **1993**, *98*, 1358.
[15] M. Dolg, H. Stoll, H. Preuss, R. M. Pitzer, *J. Phys. Chem.* **1993**, *97*, 5852.
[16] P. Pyykkö, N. Runeberg, F. Mendizabal, *Chem. Eur. J.* **1997**, *3*, 1451.
[17] G. D. Purvis, R. J. Bartlett, *J. Chem. Phys.* **1982**, *76*, 1910.
[18] K. Raghavachari, G. W. Trucks, J. A. Pople, M. Head-Gordon, *Chem. Phys. Lett.* **1989**, *157*, 479.
[19] R. J. Bartlett, J. D. Watts, S. A. Kucharski, J. Noga, *Chem. Phys. Lett.* **1990**, *165*, 513.
[20] F. Weigend, M. Häser, *Theor. Chem. Acc.* **1997**, *97*, 331.
[21] F. Weigend, M. Häser, H. Patzelt, R. Ahlrichs, *Chem. Phys. Lett.* **1998**, *294*, 143.
[22] R. Ahlrichs, M. Bär, M. Häser, H. Horn, C. Kölmel, *Chem. Phys. Lett.* **1989**, *162*, 165.
[23] G. M. Chaban, J. O. Jung, R. B. Gerber, *J. Chem. Phys.* **1999**, *111*, 1823.
[24] J. M. Bowman, *Acc. Chem. Res.* **1986**, *19*, 202.
[25] M. W. Schmidt, K. K. Baldridge, J. A. Boatz, S. T. Elbert, M. S. Gordon, J. J. Jensen, S. Koseki, N. Matsunaga, K. A. Nguyen, S. Su, T. L. Windus, M. Dupuis, J. A. Montgomery, *J. Comput. Chem.* **1993**, *14*, 1347.
[26] *Handbook of Chemistry and Physics* (Ed.: D. R. Lide), 80th ed., CRC Press, **2002**.
[27] A. Schäfer, A. Klamt, D. Sattel, J. C. W. Lohrenz, F. Eckert, *Phys. Chem. Chem. Phys.* **2000**, *2*, 2187.
[28] M. N. Akhtar, A. A. Isab, A. R. Al-Arfaj, M. S. Hussain, *Polyhedron* **1997**, *16*, 125.
[29] A. L. Hormann, C. F. Shaw III, D. W. Bennett, W. M. Reiff, *Inorg. Chem.* **1986**, *25*, 3953.
[30] Y. Pak, R. C. Wood, K. A. Peterson, *J. Chem. Phys.* **1995**, *103*, 9304.
[31] M. Polak, M. Gruebele, R. J. Saykally, *J. Chem. Phys.* **1987**, *87*, 3352.
[32] D. F. Smith Jr, *J. Mol. Spectrosc.* **1975**, *57*, 447.
[33] P. Pyykkö, *Angew. Chem.* **2004**, *116*, 4512; *Angew. Chem. Int. Ed.* **2004**, *43*, 4412.
[34] H. Schmidbaur, A. Hamel, N. W. Mitzel, A. Schier, S. Nogai, *Proc. Natl. Acad. Sci. USA* **2002**, *99,* 4916, and references therein.
[35] T. Mathieson, A. Schier, H. Schmidbaur, *J. Chem. Soc. Dalton Trans.* **2001**, 1196.
[36] G. Lewis, C. F. Shaw III, *Inorg. Chem.* **1986**, *25*, 58.
[37] A. L. Hormann-Arendt, C. F. Shaw III, *Inorg. Chem.* **1990**, *29*, 4683.
[38] M. N. Akhtar, I. H. Ghazi, A. A. Isab, A. R. Al-Arfaj, M. I. M. Wazeer, M. S. Hussain, *J. Coord. Chem.* **1995**, *36*, 149.
[39] N. J. de Stefano, J. L. Burmeister, *Inorg. Chem.* **1971**, *10*, 998.
[40] M. M. El-Etri, W. M. Scovell, *Inorg. Chem.* **1990**, *29*, 480.
[41] J. L. Burmeister, J. B. Melpolder, *J. Chem. Soc.* **1973**, 613.
[42] J. B. Melpolder, J. L. Burmeister, *Inorg. Chim. Acta* **1981**, *49*, 115.
[43] R. G. Pearson, *Inorg. Chem.* **1973**, *12*, 712.
[44] A. E. Elia, E. C. Lingafelter, V. Schomaker, *Acta Crystallogr.* **1984**, *40*, 1313.
[45] E. O'Grady, N. Kaltsotannis, *Phys. Chem. Chem. Phys.* **2004**, *6*, 680.

Received: September 7, 2004
Published online: April 1, 2005